JOURNAL OF GEOPHYSICAL RESEARCH, VOL. 101, NO. A2, PAGES 2453–2460, FEBRUARY 1, 1996

The self-focusing instability in the presence of density irregularities in the ionosphere

P. N. Guzdar, P. K. Chaturvedi, and K. Papadopoulos
Institute for Plasma Research, University of Maryland, College Park

M. J. Keskinen and S. L. Ossakow
Plasma Physics Division, Naval Research Laboratory, Washington, D. C.

Abstract. The self-focusing instability of high-power radio waves in the ionosphere in the presence of density irregularities is presented. The present study addresses the role of preexisting density irregularities which are always present in the instability region. The presence of ambient irregularities results in the excitation of wave numbers, which, on the basis of homogeneous theory of the self-focusing instability, should be stable. This effect can explain the puzzling observations that indicate growth of the medium-scale (on the order of hundreds of meters) irregularities during ionospheric heating. The computational results are compared with available experimental data and will be used to plan experiments using the upcoming High-Frequency Active Auroral Research Program heater.

1. Introduction

The ionospheric modification experiments using radio frequency (RF) heater facilities at Arecibo, Platteville, Alaska, the SURA facility in Russia, and Tromso provide a rich variety of results related to the spatial structures in the ionospheric medium, the scattered electromagnetic signals, and particle energization [*Litvak*, 1970; *Carlson and Duncan*, 1977; *Carlson et al.*, 1982; *Stubbe et al.*, 1982; *Fejer et al.*, 1985; *Erukhimov et al.*, 1987; *Wong et al.*, 1989]. These experiments have shown that increases in HF power results in the predominance of nonlinear effects, e.g., the self-focusing instability [*Litvak*, 1970; *Perkins and Valeo*, 1974; *Cragin et al.*, 1977; *Gurevich*, 1978; *Perkins and Goldman*, 1981; *Bernhardt and Duncan*, 1982, 1987]. Observations made with ionosondes [*Utlaut*, 1970], scintillation studies [*Thome and Perkins*, 1974; *Basu et al.*, 1983, 1987], radar scattering [*Duncan and Behnke*, 1978; *Frey et al.*, 1984], in situ satellite measurements [*Farley et al.*, 1983], optical emissions [*Bernhardt et al.*, 1988], dynasonde HF radar [*Wright et al.*, 1988], and in situ rocket measurements [*Kelley et al.*, 1995] have revealed the excitation of irregularities in the medium during the RF (radio wave) heating experiments, which have been attributed to the self-focusing instability (SFI). The self-focusing (and filamentation) instability has also been of interest in various other plasma environments, such as the laser plasma interaction studies. There have been some recent reports of observations of the filamentation instability (in the underdense region) in the laser-plasma interaction experiments [*Young*, 1991, and references therein]. Theories have often been successful in explaining certain observational features. There are, however, several puzzling observations and associated scientific controversies. For example, the observations often indicate the generation of medium scale size (tens to hundreds of meters) irregularities for typical pump powers, while the theoretical estimates predict longer scales (kilometers) for these power levels. Current theoretical models overestimate the thresholds for excitation of the observed scales by an order of magnitude [*Farley et al.*, 1983; *Frey et al.*, 1984; *Frey and Duncan*, 1984].

Current theories emphasize identification of the physical processes leading to self-focusing in homogeneous plasmas. They have often not considered many realistic effects, such as density irregularities in the medium. These nonideal factors affect the self-focusing instability, because they affect the local refractive index of the plasma. In the present paper we study the self-focusing of radio waves in the ionosphere for the underdense (pump frequency, ω_0, much greater than the plasma frequency, ω_{pe}) case in two dimensions (2D). The 2D geometry captures the essential physics aspects of the self-focusing instability. We find that the presence of density irregularities in the medium results in simultaneous excitation of the self-focusing instability at short and long wavelengths due to mode coupling. This broadband excitation occurs for threshold pump powers for which the homogeneous plasma theory predicts excitation of long wavelengths only. The mechanism is akin to the quasi-resonant mode coupling excitation of high-k wavenumbers by long-wavelength Langmuir waves in the presence of sinusoidal density perturbations [*Kaw et al.*, 1973b]. These results provide a natural explanation for the observations of small scale sizes at low pump powers [*Frey et al.*, 1984; *Frey and Duncan*, 1984]. We note that the validity of the analysis in the underdense regime is to within an Airy scale length (determined by the plasma inhomogeneity) of the critical surface and hence has a broader range of applicability close to the overdense situation. *Bernhardt and Duncan* [1982] have carried out 2D numerical simulations of the self-focusing instability. They included an initial sinusoidal perturbation of the density in the case of underdense plasma when the pump wave was represented by a plane wave. This density perturbation leads to the linear growth of the self-focusing instability (SFI) at the same wavelength. Their results for this case showed that the initial pattern evolved into a distorted pattern (due to nonlinear effects) with smaller scale sizes. We examine analytically

Paper number 95JA02975.
0148-0227/96/95JA-02975$02.00

and numerically the influence of the presence of a short-wavelength sinusoidal irregularity mode on the unstable k spectrum and on the thresholds of the SFI. For a uniform pump the SFI would be absent at these (short) scale sizes. However, with a nonuniform pump of much longer wavelength the instability grows not only at the long wavelength but also at shorter wavelengths because of sideband coupling with the ambient short scale length density fluctuation. In view of the planned upgrading of the existing ionospheric heater facilities, and the planned enhanced power facility like the High-Frequency Active Auroral Research Program (HAARP), the results will be of relevance and interest for applications to communication and remote sensing (K. Papadopoulos et al., unpublished manuscript, 1995).

The paper is organized as follows. The analysis of the collisional self-focusing instability in the presence of density irregularities is presented in the next section. The third section discusses the numerical results. The fourth section presents the results of a marginal stability analysis. The last section includes a comparison of the theory with observations and a summary of the paper.

2. The Self-Focusing Instability

We present first a simplified picture of the self-focusing instability which includes the effects of the density irregularities in the medium. In the collisional case the important nonlinear effect is the thermal nonlinearity (nonlinear Joule heating). In this case the regions of higher field intensity experience enhanced temperature as a result of the increased resistive heating, and the resulting hydrodynamic expansion of the plasma causes the plasma density to be reduced in the elevated temperature regions (enhanced field intensity regions). The resultant modification in the nonlinear dielectric constant of the medium tends to focus the beam in the depleted density regions, resulting in an instability. An isothermal equation of state, $p = nT$, cold ions ($T_i = 0$), and $\nu_e \approx \nu_{ei}$ are assumed. By considering scale sizes large enough, thermal conductivity effects can be neglected in comparison with the electron cooling effects due to collisions with ions. We consider a situation in which the electromagnetic (EM) beam enters a plasma which has a sinusoidal equilibrium density modulation and then examine the stability of the beam to perturbations with wave number different from the density irregularity. We describe the equilibrium density as

$$n_{0m}(y) = n_0(1 - \varepsilon_i \cos k_i y), \tag{1}$$

where n_{0m} denotes the modified equilibrium density, n_0 is the undisturbed ambient density, and ε_i, k_i are the amplitude and wave number of the density irregularity. We have assumed that there is no variation in the ambient density fluctuations along the direction of propagation (z). This is justified, since in the high-latitude ionosphere, the region on which our study is focused, the vertical direction, the z axis, is nearly aligned with the ambient magnetic field. The instability mechanism responsible for the natural density irregularities (such as the interchange mode [*Chaturvedi et al.*, 1992]) preferentially excites modes which are highly elongated along the field lines, and $L_\parallel \gg \lambda_\parallel$ is satisfied (here, $L_\parallel$ and $\lambda_\parallel$ are the parallel scale lengths associated with the interchange and self-focusing instabilities, respectively). We consider the situation of a large-amplitude EM wave propagating along the z axis, $\mathbf{E} = \mathbf{E}_0 \cos(\omega_0 t - k_0 z)$. As shown in the work of *Kaw et al.* [1973a], in thermal equilibrium the nonlinear dielectric constant, ζ, for an unmagnetized plasma in the presence of the wave is

$$\zeta(\langle E^2 \rangle) = 1 - \frac{\omega_{pe}^2}{\omega_0^2} \exp[-\beta \langle E^2 \rangle]. \tag{2}$$

where $\omega_{pe} = (4\pi n_0 e^2/m_e)^{1/2}$ is the electron plasma frequency, ω_0 is the EM wave frequency, $\beta = -e^2/2m_e\omega_0^2(T_e + T_i)$, T_e, T_i are the electron and ion temperatures (in energy units), respectively, and $\langle E^2 \rangle$ is the time-averaged intensity of the incident HF wave. We choose $\mathbf{E}_0 = \hat{e}_x E_0$ and perturb the equilibrium, with perturbations of the form

$$\delta\mathbf{E} = \mathbf{e}_{1x}(\mathbf{x}) \cos(\omega_0 t - k_0 z) + \mathbf{e}_{2x}(\mathbf{x}) \sin(\omega_0 t - k_0 z). \tag{3}$$

Expanding ζ, the nonlinear dielectric constant around the uniform beam intensity, $(\langle E_0^2/2 \rangle)$ (neglecting second-order terms), leads to the perturbed components of the wave equations [*Kaw et al.*, 1973a]

$$-2k_0 \frac{\partial e_{2x}}{\partial z} + \nabla^2 e_{1x} - \left(\frac{\omega_{pe}^2}{c^2} \varepsilon_i \cos k_i y \right) e_{1x} = \frac{\omega_0^2}{c^2} \frac{n_0}{n_c} E_0 \frac{n_1}{n_0}. \tag{4}$$

$$2k_0 \frac{\partial e_{1x}}{\partial z} + \nabla^2 e_{2x} - \left(\frac{\omega_{pe}^2}{c^2} \varepsilon_i \cos k_i y \right) e_{2x} = 0. \tag{5}$$

In the above, n_c is the critical plasma density (where $\omega_0 = \omega_{pe}$), and $n_0/n_c < 1$ (underdense plasma). The energy balance equation for electrons is used to compute the temperature perturbations, while the density perturbations are computed by using the continuity and momentum transfer equations [*Gurevich*, 1978]. The equation for the low-frequency density fluctuation, in the "quasi-static" limit, is

$$\frac{n_1}{n_0} = -\frac{1}{\delta} \frac{v_{osc}^2}{v_{te}^2} \left(\frac{\mathbf{e}_1 \cdot \mathbf{E}_0}{E_0^2} \right). \tag{6}$$

where $n_1 = n - n_0$, $v_{osc}^2 = (e^2 \langle E_0^2 \rangle / 2m_e^2\omega_0^2)$, $v_{te} = (T_e/m_e)^{1/2}$, and $\delta = 2(m_e/m_i)$ is the fraction of energy lost by an electron in collisions with ions. The inelastic collisional cooling mechanisms, like the rotational, vibrational, or the fine structure excitations, and the recombination damping are more likely to be of importance at lower altitudes (<200 km) and hence have not been included here. The neglect of the electron thermal conductivity sets a lower limit on the validity of the wavelengths at which the treatment is valid. For ~250-km altitude this limit implies that the treatment is valid for transverse scales, $L_\perp > 20$ m, and the parallel scales, $L_\parallel > 30$ km. (In making these estimates we have assumed $T_e = 0.1$ eV, $\nu_{ei} = 5 \times 10^3$ s^{-1}. The inclusion of the other loss mechanisms would renormalize the coefficient in equation (6) of the loss term but would not alter the basic results of the analysis.) The additional assumption used in deriving these equations is that the growth length in the direction of propagation is much longer than k_0^{-1}, so that the second derivative term in z is negligible. This assumption is valid in the underdense plasma. In the absence of equilibrium nonthermal density irregularities the dispersion relation obtained from equations (4)–(6) is [*Gurevich*, 1978]

$$4k_0^2k_z^2 = -k_y^2\left[k_y^2 - \frac{1}{\delta}E_0^2\zeta'\left(\frac{\omega_0^2}{c^2}\right)\right] = -k_y^2\left[k_y^2 - \frac{1}{\delta}\frac{\omega_{pe}^2}{c^2}\frac{v_{osc}^2}{v_{ie}^2}\right]. \quad (7)$$

In deriving equation (7), growing solutions in the z direction of the form $\exp(k_z z + ik_y y)$ were assumed, and $\zeta' = \partial\zeta/\partial\langle E^2\rangle$. The perturbation in the y direction can be viewed as the modulation on the pump intensity, and k_z is the inverse of the convective growth length along the direction of propagation. Instability occurs for

$$E_0^2\left(\frac{\zeta'}{\delta}\frac{\omega_0^2}{c^2}\right) > k_y^2 \quad (8)$$

or

$$k_0^2\left(\frac{n_0}{n_c}\right)\left(\frac{v_{osc}^2}{c_s^2}\right) > k_y^2. \quad (9)$$

where n_c is the critical plasma density (as defined after equation (5)) and, $c_s^2 = (2T/m_i)$, $T_e = T_i = T$, and $\omega_0 = ck_0$ (free space value) have been assumed. It is readily seen that the instability favors large transverse scale sizes. This is because the diffraction effects become stronger at short wavelengths and suppress focusing. The inclusion of effects such as ion-neutral collisions and thermal conductivity effects is needed for a more accurate estimation of realistic power thresholds required for the instability in the ionosphere [*Perkins and Goldman*, 1981].

The presence of density irregularities with wave number k_i leads to a generation of sidebands ($k \pm k_i$), with the perturbed fields $e_{1x(k\pm k_i)}$, $e_{2x(k\pm k_i)}$. The perturbed fields $e_{1x(k\pm k_i)}$, $e_{2x(k\pm k_i)}$ in turn couple to modes $e_{1x(k\pm 2k_i,k)}$, $e_{2x(k\pm 2k_i,k)}$, and so on. We present numerical solutions of the set (4)–(6) obtained using the "splitting" scheme [*Press et al.*, 1986].

3. Numerical Results

By using equation (6), equations (4) and (5) can be written in dimensionless form as

$$-\frac{\partial\hat{e}_2}{\partial\hat{z}} + \frac{\partial^2\hat{e}_1}{\partial\hat{y}^2} + (\varepsilon_d\cos\hat{k}_i\hat{y})\hat{e}_1 + \alpha\hat{e}_1 = 0 \quad (10)$$

$$\frac{\partial\hat{e}_1}{\partial\hat{z}} + \frac{\partial^2\hat{e}_2}{\partial\hat{y}^2} + (\varepsilon_d\cos\hat{k}_i\hat{y})\hat{e}_2 = 0, \quad (11)$$

where

$$\hat{e} = \frac{e}{E_0} \qquad \hat{z} = \frac{z}{z_0} \qquad \hat{y} = \frac{y}{y_0} \qquad \hat{k} = ky_0$$

$$\alpha = \left(\frac{\omega_0^2}{c^2}\right)\left(\frac{z_0}{2k_0}\right)\left(\frac{n_0}{n_c}\right)\frac{1}{\delta}\left(\frac{v_{osc}^2}{v_{ie}^2}\right) \quad (12)$$

$$z_0 = 2k_0y_0^2 \qquad \varepsilon_d = \frac{\omega_{pe}^2 z_0}{2c^2k_0}\varepsilon_i,$$

and y_0 and z_0 are the characteristic scales in the y and z directions determined by the system parameters. The subscripts and carets are dropped in the following for simplicity. We discuss below three cases of growth of the self-focusing instability.

We first consider a homogeneous plasma ($\varepsilon_d = 0$). Figure 1 shows the developed stage of the instability for beam intensity corresponding to $\alpha = 1.1$ and $k_y = 1$. The perturbed electric field intensity, $|e_1|^2$, in real space (Figure 1a) and in Fourier space (Figure 1b), is plotted. In Figure 1c the growth of the maximum (in y) of the perturbed intensity as a function of z is plotted. The numerical calculations were performed so as to compute the growth of the perturbed beam intensity in z for a given value of k_y and α. For $k_y = 1$ and $\alpha > 1$ this growth rate computed by the code agrees with that obtained from the dispersion relation in equation (7). Also we see from Figures 1a and 1b that a single Fourier mode with $k_y = 1$ ($\lambda_y \sim 2.5$ km) is the natural eigenmode of the equations. (Note that the k_y above has been normalized with respect to y_0, and the corresponding wavelength is therefore $\lambda_y = (2\pi y_0/k_y)$). We note that for the parameters considered in the computations, namely, $f_0 \sim 5$ MHz, $k_0 \sim 10^{-3}$ cm^{-1}, $\alpha \geq 1$, and for a pump power density value of $I \simeq 2$ μW m^{-2} the characteristic scales y_0 and z_0 are 440 m and 38 km, respectively. The pump power intensity of $I \simeq 2$ μW m^{-2} corresponds to $v_{osc}/c_s \sim 0.16$, where v_{osc} is the so-called "quiver" (oscillatory) velocity of electrons under the pump electric field, $v_{osc} \sim eE_0/m_e\omega_0$, $c_s^2 = ((T_e + T_i)/m_i)$ and $T_e \sim T_i \sim T \sim 0.1$ eV. In arriving at these values we have considered the reflection altitude to be ~250 km and have used $n_0/n_c = 1/4$ (and $\nu_{in} \sim 4$) as our treatment is for the underdense case. (Often the pump powers used in experiments are larger than 2 μW m^{-2}, but excitation of irregularities for powers comparable to these has been observed [*Farley et al.*, 1983; *Kelley et al.*, 1995]. Furthermore, the threshold requirement for the self-focusing instability for the overdense case may be overestimated, especially for high latitudes [*Cragin et al.*, 1977], while our results are applicable to the underdense region where the threshold requirement is lower.) A more accurate determination of the unstable scale sizes for these power levels yields comparable values (~1 km) [*Perkins and Goldman*, 1981]. We next introduce a density perturbation, $\varepsilon_d = 5.0$, with $k_i = 4k_y$ for the same values of the pump intensity and initial k_y as in Figure 1. For plasma parameters relevant to the high-latitude ionosphere near the reflection altitude of the electromagnetic wave and a pump

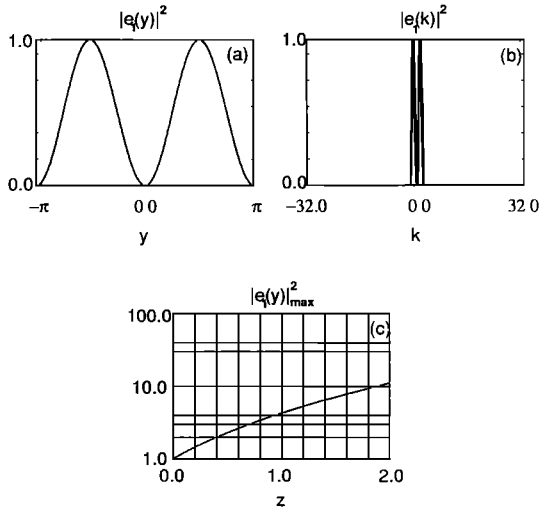

Figure 1. (a) Perturbation intensity in the configuration space $|e_1(y)|^2$ versus y, (b) perturbation intensity in Fourier space $|e_1(y)|^2$ versus k, and (c) the maximum perturbed intensity in y as a function of z, for $\alpha = 1.1$, $k_y = 1$, and $\varepsilon_d = 0$.

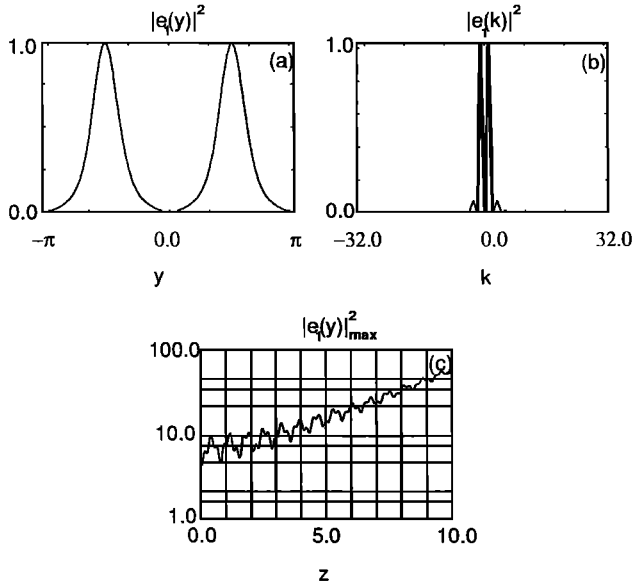

Figure 2. Same as Figure 1 but with $\varepsilon_d = 5.0$.

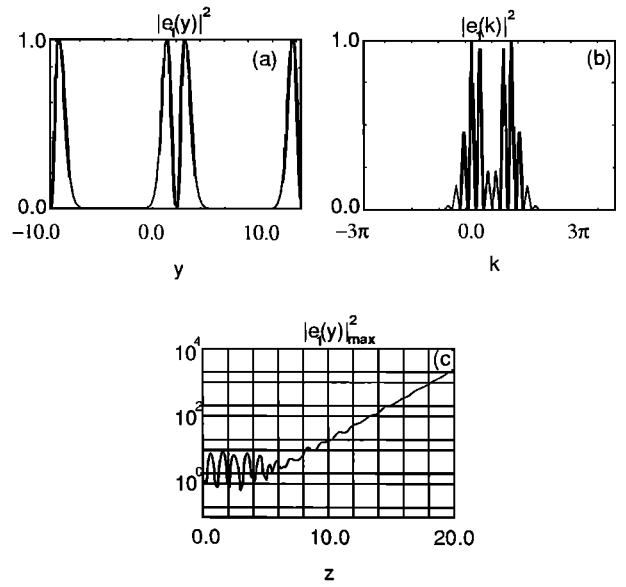

Figure 3. Same as Figure 2 but with $\alpha = 0.5$ and initial $k_y = 0.3$.

intensity of 2 μW/m^2, this value of ε_d translates into a density fluctuation of 1.7%. In Figure 2a we plot $|e_1|^2$ as a function of y, while in Figure 2b, $|e_{1k}|^2$ versus k is plotted. In Figure 2c the growth of the self-focusing mode is shown along the z axis. An initial cosinusoidal perturbation (for e_1 and e_2) evolves to the eigenmode shown in Figure 2a. This is the final "eigenmode" in the y direction. (The "wiggles" in Figure 2c, which is a plot of the maximum value of $|e_1(y)|^2_{max}$, is a consequence of "finding" the correct eigenfunction given an initial perturbation which is not an eigenstate of the equations.) The interesting feature in the k spectrum is that besides the peaks at $k = \pm 1$ present in the previous case there are additional peaks at $\pm(k_y \pm nk_t)$, with $n = 1$, i.e., at $k = \pm 3$ and ± 5. In the homogeneous case the perturbation at these mode numbers would have been stable for the specified pump intensity. Thus even if the initial modulation of the pump is a long-wavelength perturbation, in the presence of background density fluctuations, high-k sidebands develop. Since in this case the intensity in the sidebands is much smaller than the primary modes, a simple perturbation theory can be developed. We observe growth of modes in this case (though the magnitude of the growth rate is slightly reduced). As a consequence the threshold is still almost the same as in the previous case, even though the k spectrum is broader.

In Figure 3 we consider the case with $k_y = 0.3$, $k_t = 4k_y$, $\alpha = 0.5$, and $\varepsilon_d = 5.0$. For a homogeneous plasma, only modes with $k_y < 0.707$ are unstable at this value of the pump intensity. In the presence of the density perturbation, significant growth for a broad band in k space is observed. Higher wave numbers, $k_y = 3.0$, substantially larger than the initial perturbation wave number $k_y = 0.3$ of the electric field as well as $k_t = 1.2$ of the ambient density irregularity, are observed. Also the highest k in the spectrum is 4 times larger than that predicted by the linear ($k_y = 0.707$) instability in the absence of density irregularities. In the present example for the given pump threshold, homogeneous plasma theory predicts instability at ($k^{-1} \sim 1$ km) and stability for $(k + 3k_i)^{-1}$ (~75 m). (These estimates may be arrived at from equation (7) or from the more accurate analysis which includes ν_{in} and thermal conductivity effects [*Perkins and Goldman*, 1981] and yields comparable values.) One finds that the excitation of $\lambda_\perp \sim 100$ m requires pump powers which are an order of magnitude higher than those required for the excitation of $\lambda_\perp \sim$ km. This example illustrates that the presence of a modest (1.7% amplitude) density fluctuation drives higher k values to instability. Thus an initial long-wavelength perturbation $k_y = 0.3$ can undergo a strong self-focusing instability and generate multiple sidebands $k_y \pm nk_t$ as the beam propagates through a medium with a density irregularity. For this case, however, the sideband intensities are large. Since there is no small parameter, an analytical theory in this regime is difficult.

The above results indicate excitation of a broadband spectrum by the self-focusing instability in the presence of a modest level of density irregularities for threshold pump powers characteristic of the linear long scale length excitation. This may explain the observed irregularities at short and long wavelengths simultaneously in the ionospheric heating experiments [*Frey et al.*, 1984; *Kelley et al.*, 1995]. The results described above are for a sinusoidal equilibrium density perturbation with a given wave number. Extension to the case of nonsinusoidal perturbation, or to the case of random perturbations, is of interest, since this is the likely form of the inhomogeneities encountered in the ionosphere. It may be noted here that the nearly simultaneous excitation of small wavelengths due to the presence of density irregularities is qualitatively similar to the quasi-resonant mode coupling of Langmuir waves in a plasma with density irregularities discussed by *Kaw et al.* [1973b]. They showed that in the presence of a sinusoidal density irregularity, long-wavelength plasma waves drove short-wavelength modes which could then exchange energy with particles via wave-particle interaction, leading to production of energetic tails.

4. Marginal Stability Analysis

In this section we show that the numerical results obtained in the preceding section are reproduced by a simplified analytic model using marginal stability analysis. In this case we assume $\partial/\partial z \approx 0$ in equations (10) and (11); then the perturbed field equations may be combined to yield

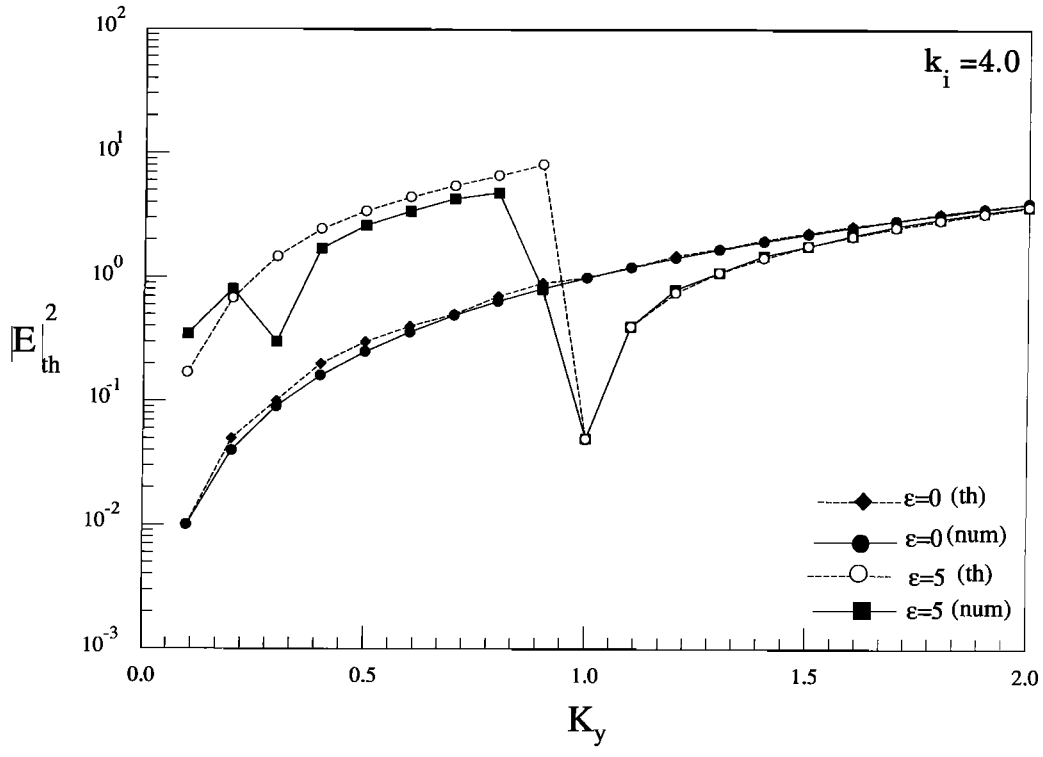

Figure 4. Power threshold for the self-focusing instability as a function of k_y, shown from analytical and numerical computations. Parameters used are for a homogeneous plasma ($\varepsilon = 0$) (analytical (dashed line with diamonds) and numerical (solid line with dark circles)), and for the case of density irregularities, $\varepsilon = 5.0$, $k_i = 4.0$ (analytical (dashed line with light circles) and numerical (solid line with squares)). (Here $\varepsilon \equiv \varepsilon_d$, and $|E|^2_{th} \equiv \alpha_T$.)

$$\frac{\partial^2 e_1}{\partial y^2} + (\varepsilon_d \cos k_i y + \alpha_T) e_1 = 0. \tag{13}$$

where $\alpha_T \propto f(|E_0|^2_T)$ and $|E_0|^2_T$ is the threshold pump intensity at the marginal stability level. We consider $e_1 = e_{10} \exp(iky) + e_{1+} \exp(i(k + k_i)y) + e_{1-} \exp(i(k - k_i)y)$. Note that we have chosen to limit the mode coupling to the first sideband only. This is justifiable near the marginal threshold condition. (The analysis may readily be extended to include higher sidebands.) The coupled equations are

$$(k^2 - \alpha_T) e_0 = \left(\frac{\varepsilon_i}{2}\right)(e_- + e_+) \tag{14}$$

$$[(k + k_i)^2 - \alpha_T] e_+ = \frac{\varepsilon_i}{2} e_0 \tag{15}$$

$$[(k - k_i)^2 - \alpha_T] e_- = \frac{\varepsilon_i}{2} e_0 \tag{16}$$

The threshold field is obtained from the determinant of (14)–(16),

$$(k^2 - \alpha_T)(k_+^2 - \alpha_T)(k_-^2 - \alpha_T) = \frac{\varepsilon_i^2}{2}(k^2 + k_i^2 - \alpha_T). \tag{17}$$

where the above analysis is valid for, $e_\pm/e_0 = \varepsilon_i/[2(k_\pm^2 - \alpha_T)] \ll 1$, so as to truncate the coupling to the first sideband.

The threshold, α_T, as a function of k, computed from expression (17), is plotted in Figures 4–6, along with the value of the threshold obtained by solving the exact set (10)–(11) numerically. In Figure 4 we find that the theoretically computed threshold (dashed lines with light circles), though obtained approximately as discussed above, agrees well with the numerical plot (solid line with squares) for the value of $\varepsilon_d = 5.0$. For comparison the thresholds from the two approaches are also plotted in this figure for the homogeneous case ($\varepsilon_d = 0.0$). The analytical thresholds (dashed line with diamonds) and numerical thresholds (solid line with dark circles) are found to agree quantitatively, as expected. In Figure 5 the thresholds, computed from (17), are plotted for the values of $\varepsilon_d = 1.0$ (solid line with dark circles), 3.0 (solid line with light circles), and 5.0 (solid line with diamonds). It is found that an increase in the ambient density fluctuation levels leads to a shift in k space toward higher k values and a decrease of threshold in this model. As in the previous case, for comparison, the case with, $\varepsilon_d = 0$, is also shown (dashed line with squares). In Figure 6 the threshold is plotted for different values of the ambient irregularity wave number, $k_i = 2.0$ (solid line with dark circles), 5.0 (solid line with light circles), and 10.0 (solid line with diamonds) for $\varepsilon_d = 3.0$. Also, the case of $\varepsilon_d = 0$ (dashed line) is shown for comparison. It is seen that for lower k_i the reduction in threshold at high k values is more pronounced, whereas for higher k_i, not only is the threshold is not much reduced for high k, but it is also increased for lower k. It may be noted here that all three cases above assumed equal density amplitudes, though it is expected that higher k_i would have lower density amplitudes and thus the increase at low k in Figure 6 for higher k_i may not be true in a realistic situation. The band structure seen in Figures 4–6 is reminiscent of the energy band structure of the electron states in a periodic lattice and is an artifact of the periodic density irregularity chosen.

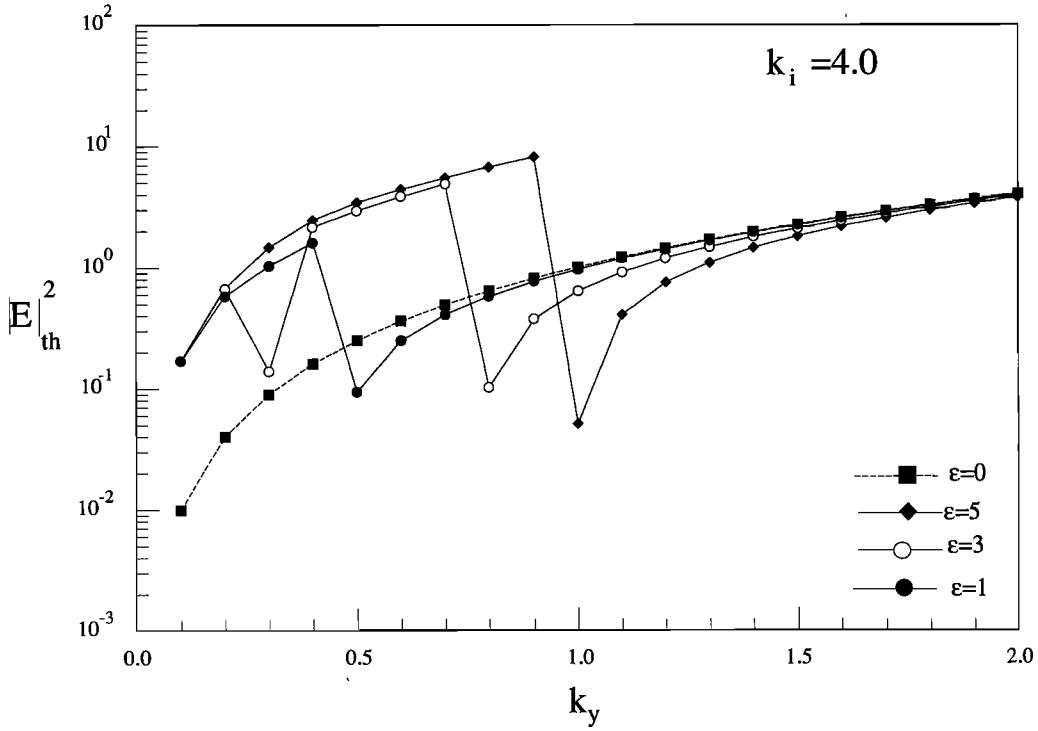

Figure 5. Similar to Figure 4 but for different $\varepsilon = 0.0$ (dashed line with squares), 1.0 (solid line with dark circles), 3.0 (solid line with light circles), and 5.0 (solid line with diamonds), with $k_i = 4.0$. (Here $\varepsilon \equiv \varepsilon_d$, and $|E|^2_{th} \equiv \alpha_T$.)

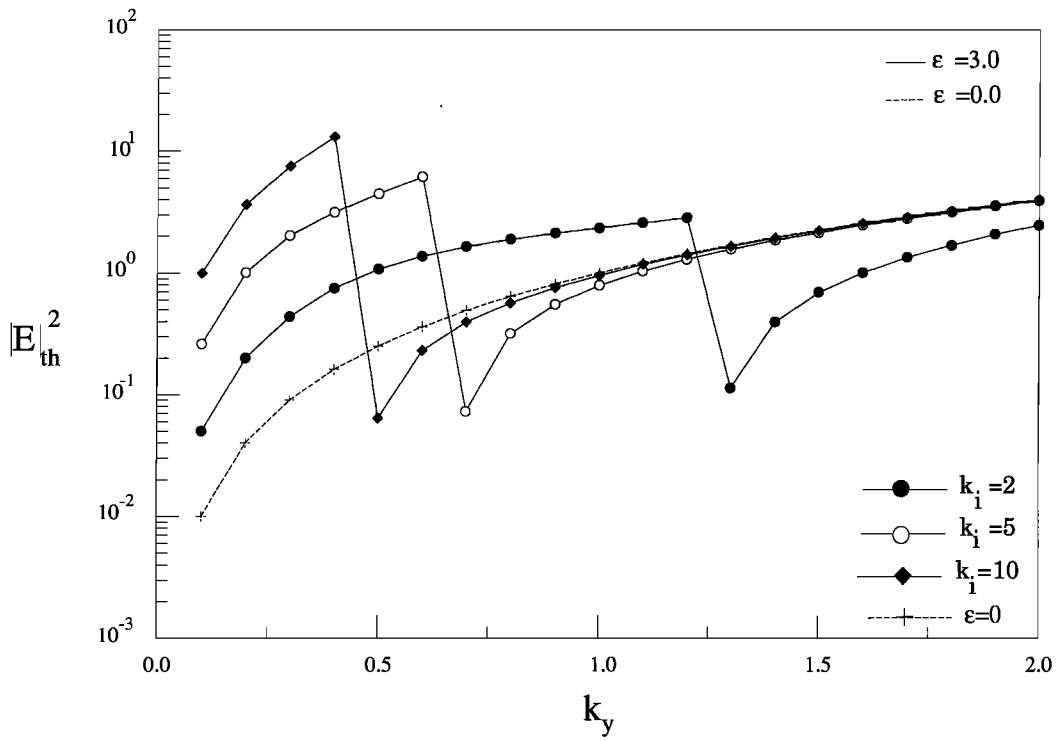

Figure 6. Similar to Figure 5 but for $k_i = 2.0$ (solid line with dark circles), 5.0 (solid line with light circles), and 10.0 (solid line with diamonds) for $\varepsilon = 3.0$ and $\varepsilon = 0.0$ (dashed line). (Here $\varepsilon \equiv \varepsilon_d$, and $|E|^2_{th} \equiv \alpha_T$.)

The physical reason for the jumps in the threshold (in Figures 4–6) at very specific mode numbers and given amplitude of the density fluctuations is as follows. When the dispersion effects are cancelled by the focusing effects of the density fluctuations, a minimum in the intensity threshold is obtained ($\alpha_T \rightarrow 0$). From the theory the value of k for which this occurs is given by

$$k^2(k + k_i)^2(k - k_i)^2 = \frac{\varepsilon_i^2}{2}(k^2 + k_i^2) \qquad (18)$$

This expression readily reproduces the dominant decrease in the threshold observed in the figures.

5. Discussion

The ionosphere is seldom quiescent, and the turbulence embedded in it is known to span a wide range of values in time, space, and amplitude. The importance of density irregularities on the parametric mode-coupling process has been demonstrated in the literature in a variety of contexts, such as the quasi-resonant mode coupling of small-k Langmuir waves to high-k Langmuir waves [*Kaw et al.*, 1973b] and the effect of random inhomogeneities on the parametric scattering processes [*Guzdar et al.*, 1974]. We have described above our preliminary study on the effect of a sinusoidal plasma density variation on the thermal self-focusing instability for the underdense case. We find that small scale sizes are excited owing to the presence of modest amplitude density irregularities by the self-focusing process for pump intensities that are subthreshold for the homogeneous case. In many ionospheric heating experiments conducted for the overdense case the observed irregularity scale sizes were such that these would be stable according to the homogeneous theory [*Frey et al.*, 1984; *Frey and Duncan*, 1984]. The homogeneous plasma theory favors excitation of longer scale sizes (greater than kilometers, for a typical pump power density level of several tens of $\mu W/m^{-2}$ used in some of these experiments [e.g., *Frey et al.*, 1984]), while the observed scale sizes were of the order of several hundreds of meters, which would have required an order of magnitude, or higher, larger pump power density values based on the uniform plasma theory. Thus the results of the present work, i.e., the excitation of small and large wavelengths simultaneously in the presence of modest density fluctuations, may provide an explanation of small scale sizes observed during the "sub-threshold" pump intensities during many ionospheric heating experiments.

It is well known that medium scale size structures are often observed in the ionosphere (more frequently at high and low latitudes) owing to natural plasma turbulence arising from low-frequency instabilities such as the interchange mode. (At midlatitudes (e.g., Arecibo), where natural processes are not known to lead to strong plasma irregularities as at high and low latitudes, the observations from heating experiments indicate formation of small-scale irregularities on "intermediate" timescales of milliseconds to seconds, resulting presumably from the "early" timescale (less than milliseconds) processes (like strong langmuir turbulence.)) A self-consistent treatment describing the self-focusing instability in the presence of ionospheric irregularities would include equations describing the "natural modes" (responsible for the irregularities) along with the equations describing the SFI. In this description the damping associated with the "natural modes" would be introduced in the coupled system describing the SFI and the "natural modes." This introduction would lead to a modification of the thresholds for the SFI. In the present work we have included only the description of the SFI in the presence of developed ionospheric irregularities, a treatment valid for the "late" time (timescales greater than seconds) regime. At both the middle and high latitudes one may expect to obtain well-developed ambient irregularities in the late timescale regime, either as a result of the "conditioning" due to the "early" time processes (at midlatitudes) or due to the "natural" modes at the high latitudes. Therefore the physical process described in the present work is expected to occur at both the middle and high latitudes in the "late" time regime. The self-consistent treatment, involving a detailed description of the irregularity formation, may lead to a modification of the thresholds, but the unstable spectrum of the SFI at "late" times would be determined by the amplitude and wave number of the irregularity mode.

Recently, an experiment was conducted in which a rocket was launched through the heated region from Arecibo [*Kelley et al.*, 1995]. The in situ plasma density observations from a Langmuir probe in this experiment show a presence of irregularities at various altitudes including regions below the reflection altitude (~268.5 km). The observations indicate "bundles" of small scale size irregularities in the range of ≥10 m (slightly larger than the ion-Larmor radius). Though our theory is not strictly valid at these scale sizes and we do not attempt a broad interpretation of the observations of Kelley et al., our results nonetheless show that low pump powers (~5 $\mu W\ m^{-2}$) may not only directly excite longer scale sizes (at least kilometers) but may also generate smaller scale sizes (≤100 m) in the presence of modest density irregularities ($\delta n/n \sim 1.7\%$).

The underdense regime may also be of interest for the oblique heating case and for over-the-horizon (OTH) radar studies (K. Papadopoulos et al., unpublished manuscript, 1995). Further, in view of the planned enhanced high-power facility in Alaska under the HAARP it will be important to compare the thermal self-focusing threshold for the underdense case with other effects which may be deleterious for the pump. The results would provide useful input for the planning of the overdense experiments.

Acknowledgments. We thank Santimay Basu and P. A. Bernhardt for interest and useful discussions. This work was supported by the National Science Foundation under grant ATM-9412848 and by the Office of Naval Research.

The Editor thanks M. P. Sulzer and P. Stubbe for their assistance in evaluating this paper.

References

Basu, S., Su. Basu, S. Ganguli, and W. E. Gordon, Coordinated study of subkilometer and 3-m irregularities in the *F* region generated by high-power HF heating at Arecibo, *J. Geophys. Res.*, *88*, 9217, 1983.

Basu, S., Su. Basu, P. Stubbe, H. Kopka, and J. Waaramaa, Daytime scintillations induced by high-power HF waves at Tromso, Norway, *J. Geophys. Res.*, *92*, 11,149, 1987.

Bernhardt, P. A., and L. M. Duncan, The feedback-diffraction theory of ionospheric heating, *J. Atmos. Terr. Phys.*, *44*, 1061, 1982.

Bernhardt, P. A., and L. M. Duncan, The theory of ionospheric focused heating, *J. Atmos. Terr. Phys.*, *49*, 1107, 1987.

Bernhardt, P. A., L. M. Duncan, and C. A. Tepley, Artificial airglow excited by high-power radio waves, *Science*, *242*, 1022, 1988.

Carlson, H. C., and L. M. Duncan, HF excited instabilities in space plasmas, *Radio Sci.*, *12*, 1001, 1977.

Carlson, H. C., Y. B. Wickwar, and G. P. Mantas, Observations of fluxes of suprathermal electrons accelerated in HF excited instabilities, *J. Atmos. Terr. Phys.*, *44*, 1089, 1982.

Chaturvedi, P. K., M. J. Keskinen, and S. L. Ossakow, High-latitude *F* region ionospheric interchange modes in the presence powerful radio waves, *J. Geophys. Res.*, *97*, 8559, 1992.

Cragin, B. L., J. A. Fejer, and E. Leer, Generation of artificial spread *F* by a collisionally coupled purely growing parametric instability, *Radio Sci.*, *12*, 273, 1977.

Duncan, L. M., and R. A. Behnke, Observations of self-focusing electromagnetic waves in the ionosphere, *Phys. Rev. Lett.*, *41*, 998, 1978.

Erukhimov, L. M., et al., Artificial ionospheric turbulence (review), *Radiophys. Quantum Electron.*, Engl. Transl., *30*, 156, 1987.

Farley, D. T., C. LaHoz, and B. G. Fejer, Studies of the self-focusing instability at Arecibo, *J. Geophys. Res.*, *88*, 2093, 1983.

Fejer, J. A., et al., Ionospheric modification experiments with the Arecibo heating facility, *J. Atmos. Terr. Phys.*, *47*, 1165, 1985.

Frey, A., and L. M. Duncan, Simultaneous observation of HF-enhanced plasma waves and HF-wave self-focusing, *Geophys. Res. Lett.*, *11*, 677, 1984.

Frey, A., P. Stubbe, and H. Kopka, First experimental evidence of HF produced electron density irregularities in the polar ionosphere: Diagnosed by UHF radio star scintillations, *Geophys. Res. Lett.*, *11*, 523, 1984.

Gurevich, A. V., *Nonlinear Phenomena in the Ionosphere*, Springer-Verlag, New York, 1978.

Guzdar, P. N., P. K. Kaw, Y. S. Satya, A. Sen, A. K. Sundaram, and R. K. Varma, Effect of random density fluctuations on parametric interactions in a plasma, *Plasma Phys. Controlled Fusion Res.*, 5th(2), 193, 1974.

Kaw, P. K., G. Schmidt, and T. Wilcox, Filamentation and trapping of electromagnetic radiation in plasmas, *Phys. Fluids*, *16*, 1522, 1973a.

Kaw, P. K., A. T. Lin, and J. M. Dawson, Quasiresonant mode coupling of electron plasma waves, *Phys. Fluids*, *16*, 1967, 1973b.

Kelley, M. C., et al., Density depletions at the 10-m scale induced by the Arecibo heater, *J. Geophys. Res.*, *100*, 17,367, 1995.

Litvak, A. G., Possibility of self-focusing of electromagnetic waves in the ionosphere, *Izv. Vyssh. Uchebn. Zaved Radiofiz.*, *11*, 814, 1970.

Perkins, F. W., and M. V. Goldman, Self-focusing of radio waves in an underdense ionosphere, *J. Geophys. Res.*, *86*, 600, 1981.

Perkins, F. W., and E. J. Valeo, Thermal self-focusing of electromagnetic waves in plasmas, *Phys. Rev. Lett.*, *32*, 1234, 1974.

Press, W. H., B. P. Flannery, S. A. Teukolsky, and W. T. Vetterling, *Numerical Recipes, The Art of Scientific Computing*, p. 660, Cambridge Univ. Press, New York, 1986.

Stubbe, P., et al., Ionospheric modification experiments in northern Scandanavia, *J. Atmos. Terr. Phys.*, *44*, 1025, 1982.

Thome, G. D., and F. W. Perkins, Production of ionospheric striations by self-focusing of intense radio waves, *Phys. Rev. Lett.*, *32*, 1238, 1974.

Utlaut, W. F., An ionospheric modification experiment using very high power, high-frequency transmission, *J. Geophys. Res.*, *75*, 6402, 1970.

Wong, A. Y., et al., Large-scale resonant modification of the polar ionosphere by electromagnetic waves, *Phys. Rev. Lett.*, *63*, 271, 1989.

Wright, J. W., H. Kopka, and P. Stubbe, A large-scale ionospheric depletion by intense radio wave heating, *Geophys. Res. Lett.*, *15*, 1531, 1988.

Young, P. E., Experimental study of filamentation in laser-plasma interactions, *Phys. Fluids B*, *3*, 2331, 1991.

P. K. Chaturvedi, P. N. Guzdar, and K. Papadopoulos, Institute for Plasma Research, University of Maryland, College Park, MD 20742. (e-mail: guzdar@fusion.umd.edu)

M. J. Keskinen and S. L. Ossakow, Plasma Physics Division, Naval Research Laboratory, Washington, DC 20375.

(Received June 2, 1995; revised August 30, 1995;
accepted September 25, 1995.)